The changing influences of the AMO and PDO on the decadal variation of the Santa Ana winds

You may also be interested in:

Contribution of large-scale circulation anomalies to changes in extreme precipitation frequency in the United States
Lejiang Yu, Shiyuan Zhong, Lisi Pei et al.

A dipole pattern in the Indian and Pacific oceans and its relationship with the East Asian summer monsoon
Jiayu Zheng, Jianping Li and Juan Feng

Decadal summer drought frequency in China: the increasing influence of the Atlantic Multi-decadal Oscillation
Chengcheng Qian, Jin-Yi Yu and Ge Chen

Roles of interbasin frequency changes in the poleward shifts of the maximum intensity location of tropical cyclones
Il-Ju Moon, Sung-Hun Kim, Phil Klotzbach et al.

Forcing of the wintertime atmospheric circulation by the multidecadal fluctuations of the North Atlantic ocean
Yannick Peings and Gudrun Magnusdottir

The role of external forcing and internal variability in regulating global mean surface temperatures on decadal timescales
Lu Dong and Michael J McPhaden

Sea surface temperature inter-hemispheric dipole and its relation to tropical precipitation
Cheng Sun, Jianping Li, Fei-Fei Jin et al.

Environmental Research Letters

LETTER

The changing influences of the AMO and PDO on the decadal variation of the Santa Ana winds

Andy K Li, Houk Paek and Jin-Yi Yu

Department of Earth System Science, University of California, Irvine, California, USA

E-mail: jyyu@uci.edu

Abstract

Santa Ana wind (SAW) events have great implications for the environment of Southern California, but the cause of their decadal variability has not been fully understood. We show with observational analysis that the Atlantic multi-decadal oscillation (AMO) has a stronger influence than the Pacific decadal oscillation (PDO) in modulating SAW activity through two mechanisms: the Great Basin pressure gradient mechanism, in which a strengthened Great Basin high promotes SAW activity and vice versa through the northeast–southwest pressure gradient across Southern California, and the Pacific jetstream displacement mechanism, in which a strengthened Pacific subtropical high (PSH) prohibits mid-latitude cyclones from traveling toward California, consequently encouraging SAW development and vice versa. While the AMO strengthens or weakens both the Great Basin and PSHs to strongly modulate SAW activity through these two mechanisms, the PDO strengthens one of the highs but weakens the other, causing the two mechanisms to cancel each other, producing little influence on SAW activity. A projection based on the AMO and PDO indicates that the above-average SAW activity observed since the beginning of the 21st century is likely to terminate after 2016, after which Southern California may experience an extended period of below-average SAW activity through 2030.

1. Introduction

The Santa Ana winds (SAWs) are a weather phenomenon in Southern California that occur most often during late autumn to early spring (e.g., Conil and Hall 2006). SAW events are characterized by high wind speeds, low relative humidity and high temperatures, and are well known for their ability to exacerbate fire conditions and aid in the spread of wildfires (Westerling *et al* 2004, Hughes and Hall 2010, Jin *et al* 2014). The Cedar Fire of 2003 is an example of a fire driven by the SAW, burning 273 264 acres and costing a total of $27 million (http://cdfdata.fire.ca.gov/incidents/incidents_details_info?incident_id =57). Their effect on air quality is also significant, due to aerosols from wildfires (Guazzotti *et al* 2001) and increased surface ozone concentrations from stratospheric intrusions (Langford *et al* 2015). Ocean ecosystems are also affected by the SAW through the ocean mixing and upwelling variations they induce (Hu and Liu 2003). The SAW forms under favorable synoptic conditions

characterized by high sea level pressure (SLP) over the Great Basin (e.g., Raphael 2003). This high SLP sets up a hydrostatic pressure gradient that culminates in air flowing through the topography into the Southern California region, warming adiabatically and gaining speed. The temperature contrast between the warm ocean off the coast of Southern California and the cold continent interior during the cold seasons helps amplify the terrain driven flow (Hughes and Hall 2010). The result of all these processes is a hot, dry, and high speed wind that blows through Southern California.

The interannual variation of the frequency and intensity of SAW events is known to be affected by several factors, including the internal dynamics of the atmosphere and the external forcing from climate phenomena, such as the El Niño-Southern oscillation (ENSO). Raphael (2003) found that the number of SAW events was lower than average during El Niño winters. El Niño was suggested to cause a southward shift of the Pacific jetstream that increased the number

of mid-latitude cyclones traveling towards California, which would hinder SAW development by producing stronger cyclonic surface winds to discourage SAW formation (Raphael and Mills 1996, Finley and Raphael 2007). In another study, Jones *et al* (2010) used the National Center for Environmental Prediction (NCEP) climate forecast system model to produce SAW events from various synoptic conditions and found that their results exhibited noticeable inter-annual variability. A candidate for the observed variability was the ENSO as suggested by Raphael (2003), but due to the differences in methodology and data used for SAW classification, relationships between the SAW and ENSO were difficult to determine (Jones *et al* 2010).

It is less clear if there is any decadal variation in SAW activity. An existence of such slow variation, possibly caused by anthropogenic warming or decadal modes of variability, is crucial for long term urban planning and fire management for Southern California. Hughes *et al* (2009, 2011) conducted model experiments using the Penn State/National Center for Atmospheric Research (NCAR) mesoscale model version 5 and weather research and forecasting model to show that anthropogenic warming can reduce the number of SAW events by weakening the temperature gradient between the desert and ocean. In contrast, Yue *et al* (2014) analyzed the multi-model simulations of the coupled model intercomparison project phase 3 and found that the models tend to project an increase in the number of strong SAW days in the late autumn under a global warming scenario.

Two major modes of decadal climate variability are the Pacific decadal oscillation (PDO; Mantua *et al* 1997) and the Atlantic multi-decadal oscillation (AMO; Schlesinger and Ramankutty 1994, Kerr 2000). The PDO is characterized, in its positive phase, by above-normal sea surface temperatures (SSTs) in the tropical eastern Pacific and below-normal SSTs in the North Pacific (Mantua *et al* 1997, Zhang *et al* 1997). The PDO cycles last between 20–30 years and are known to be capable of modulating climate over North America (Dettinger *et al* 1998). The AMO is characterized by slow warming and cooling phases in SSTs in the North Atlantic Ocean that last between 65–80 years (Enfield *et al* 2001). It has been shown that the AMO can impact climate not only within the Atlantic basin but also across the Northern Hemisphere, including the Pacific Ocean and North America (McCabe *et al* 2004, Zhang and Delworth 2007, Qian *et al* 2014, Yu *et al* 2015). Since it has not yet been documented, the individual influences of the PDO and AMO on SAW activity are examined in this study.

2. Data

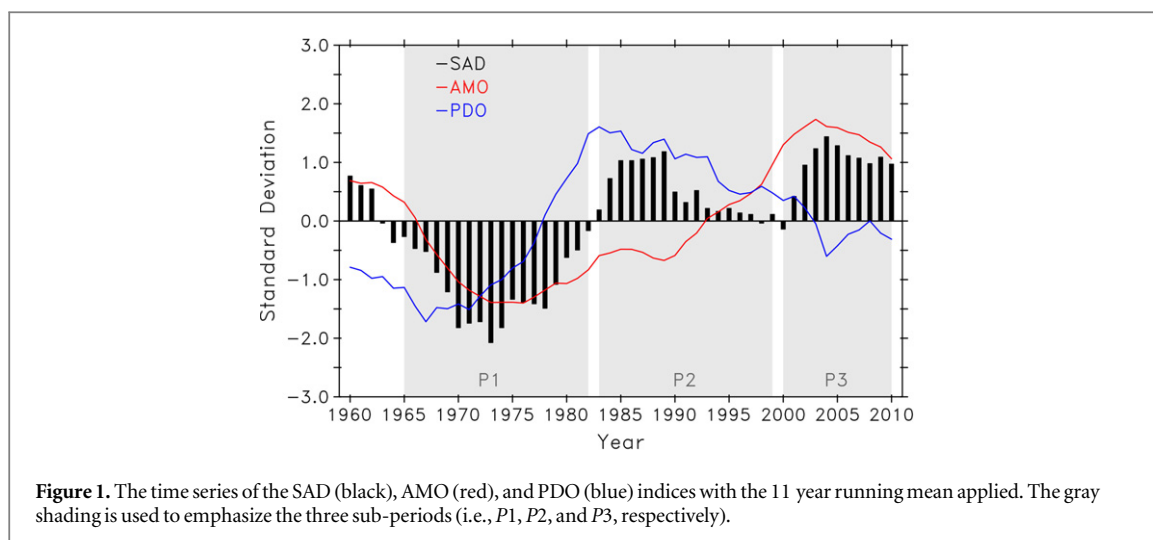The SAW dataset used for this study was constructed from the list of Santa Ana wind days (SADs) compiled by Abatzoglou *et al* (2013). The list of SAD is available at http://nimbus.cos.uidaho.edu/JFSP/pages/publications.html. To classify SAD, they used the criteria of a northeast–southwest SLP gradient across Southern California and strong cold air advection from the desert into the Transverse Range, using daily data from the NCEP/NCAR Reanalysis dataset (Kalnay *et al* 1996) from 1948 to 2010. The SAD data from Abatzoglou *et al* (2013) was chosen for this study because it covers a longer period than other SAW datasets and has been validated with known SAW events from National Climatic Data Center storm database. In this study, a SAD index was constructed by first calculating the annual means of SAD and then normalizing the annual means by their standard deviation (std). The analysis period for this study is from 1960 to 2010. In order to properly account for the number of SAD in the winter season, the annual mean of SAD in Year N, for example, is defined as the mean from July of year N to June of year $N+1$. Anomalies were defined as the deviations from the 1960–2010 climatology.

Two indices were downloaded from the National Oceanic and Atmospheric Administration (http://esrl.noaa.gov/psd/) and the University of Washington (http://research.jisao.washington.edu/pdo/) to represent the strengths of the AMO and PDO. The AMO index was calculated from the Kaplan SST dataset (Kaplan *et al* 1998) by obtaining the area-averaged SST anomalies over the North Atlantic (0°–70°N) and detrending the time series (Enfield *et al* 2001). The PDO index is defined as the leading principal component of monthly SST anomalies over the North Pacific (poleward of 20°N) (Mantua *et al* 1997). The NCEP/NCAR reanalysis dataset for the period 1960–2010 (51 years) was mainly used to provide SLP and wind information. To validate the results obtained from the NCEP/NCAR reanalysis dataset, we also used the 20th century reanalysis dataset (Compo *et al* 2011) for the period 1900–2012 (113 years). Both reanalysis datasets were obtained from http://esrl.noaa.gov/psd/.

3. Results

3.1. The decadal variation of SAW and its relationships with the AMO and PDO

The decadal variation of the SAD is examined in figure 1 by showing the 11 year running means of the SAD index. The figure indicates that the average length of SAD fluctuated by about ±2 std's (i.e., ±7.8 days year^{-1}) from the normal value (i.e., 23.6 days year^{-1}) during the past five decades. SAW activity is suppressed from early-1960 to early-1980, during which SAW activity stayed about two std's below normal. The activity became much stronger than normal in the 1980s, near normal in the 1990s, and much stronger than normal again in the first decade of the 21st

Figure 1. The time series of the SAD (black), AMO (red), and PDO (blue) indices with the 11 year running mean applied. The gray shading is used to emphasize the three sub-periods (i.e., *P*1, *P*2, and *P*3, respectively).
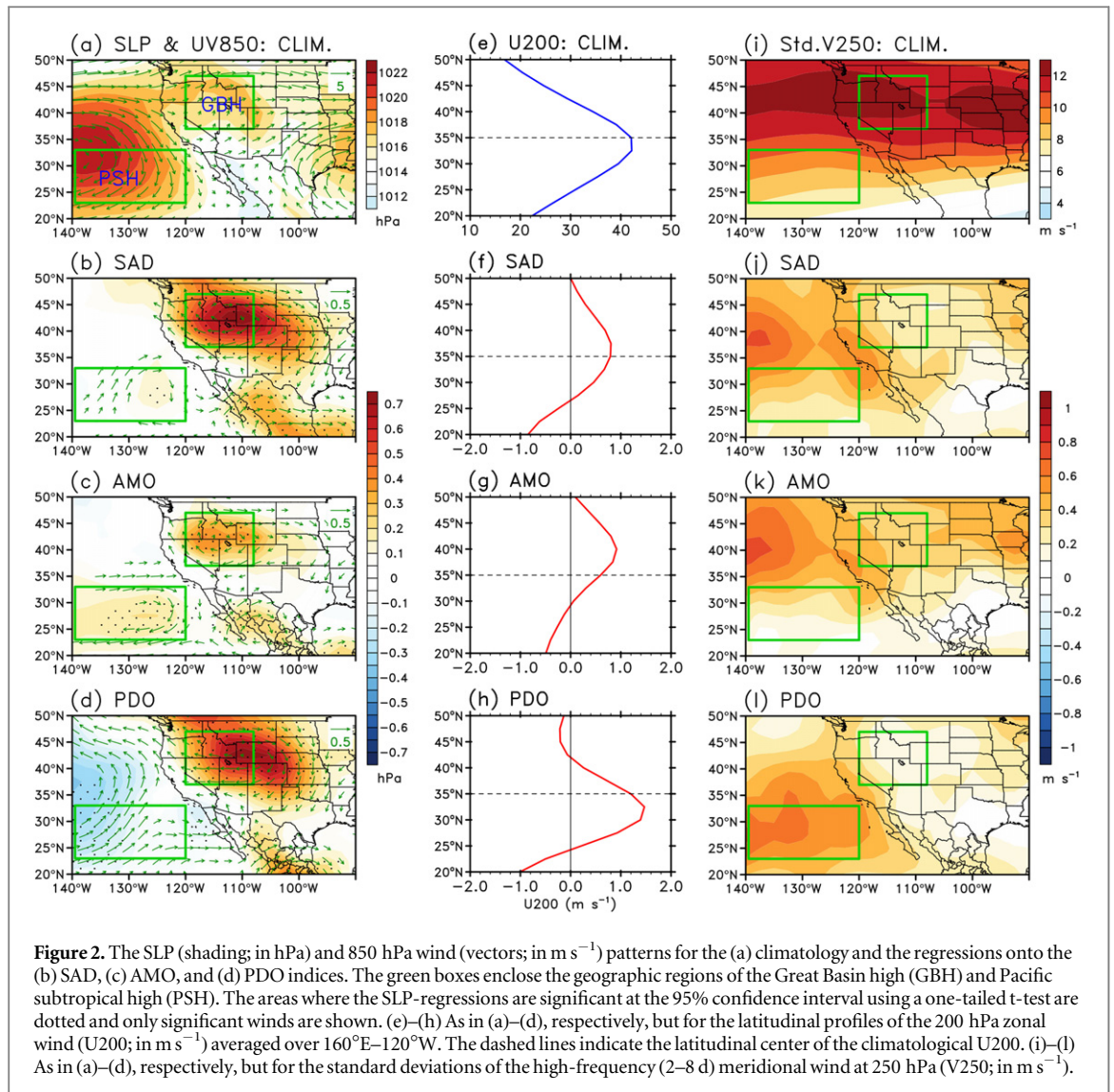
century. The ongoing decade of strong SAW activity shows little sign of decrease in SAD anomalies up until 2010. The stronger-than-normal SAW activity observed in the 21st century is opposite from the projection that anthropogenic warming may weaken SAW activity (Hughes *et al* 2009). This inconsistency raises the possibility that the variation of SAW activity in the last few decades may be related to natural decadal variability, such as the PDO or the AMO. To examine this possibility, we superimpose the time series of the AMO and PDO indices on figure 1. We find the correlation coefficient of the SAD index with the AMO index to be 0.72 and to be 0.49 with the PDO index. The difference between the correlation coefficients is significant at the 95% confidence level using a bootstrapping procedure (von Storch and Zwiers 1999) with 1000 times resampling. Alternatively, we composite the SAD index for the positive and negative phases of the AMO or PDO (i.e., years in which the indices are larger (smaller) than +0.7 (−0.7) std's) and find the composite difference to be larger between the two phases of the AMO (9.2 days year^{-1}) than that of the PDO (5.6 days year^{-1}). It is intriguing to find the decadal SAW variation to have a larger association with the decadal SST variations in the Atlantic (i.e., AMO) than with the decadal SST variations in the Pacific (i.e., PDO). The variation of the AMO index matches up well with the SAD variation in most of the analysis period, during which the value of SAD increases (decreases) when the AMO value increases (decreases). Only the period of 1983–1999 shows that the variation of the SAD follows more closely with that of the PDO.

3.2. The two mechanisms linking the AMO and PDO to the SAD variation

The connection between the decadal SAD variation and the AMO and PDO is likely linked through large-scale circulation patterns in the atmosphere, which can affect either the SLP gradient between the Great Basin and Southern California (Raphael 2003) or the

latitudinal location of the Pacific jetstream that controls the path of winter cyclones (Raphael and Mills 1996) to modulate SAW activity. We refer to the former mechanism as the Great Basin high (GBH)—pressure gradient mechanism and the latter as the Pacific subtropical high (PSH)—jetstream displacement mechanism. To explore these two hypothesized mechanisms, we regressed SLP and 850 hPa wind anomalies from the NCEP/NCAR Reanalysis dataset onto the 11 year running means of SAD, AMO, and PDO indices as shown in figure 2. For reference, the climatology of these two variables are shown in figure 2(a). For the SAD index, the regressed SLP anomaly pattern (figure 2(b)) is characterized by strong positive values over the Great Basin (outlined by a green box in the figure), which induces anti-cyclonic wind anomalies over the region and produces northeasterlies from the mountainous areas toward the southwest coast. The regressed SLP anomalies also indicate a strengthening of the PSH (also outlined by a green box in the figure) associated with above-normal SAD values. Since the associated wind anomalies off the Southern California area are either not statistically significant or are against the direction of the SAW, the strengthened PSH is unlikely to intensify SAW activity via the GBH—pressure gradient mechanism. It is more likely that the PSH—jetstream displacement mechanism links the variation of the PSH to SAW activity. A stronger PSH can push the Pacific jetstream more poleward and decrease the frequency of winter cyclones that move toward Southern California, which should favor the development of SAW activity and above-normal values of SAD. To further test this mechanism, we examine the latitudinal profile of the winter (December through February) zonal wind at 200 hPa (U200) outside North America (between 160° E–120°W) regressed onto the SAD index. We find from figure 2(f) that the U200 anomalies regressed onto the SAD index exert a northward displacement of the Pacific jetstream from its climatological location of

Figure 2. The SLP (shading; in hPa) and 850 hPa wind (vectors; in m s^{-1}) patterns for the (a) climatology and the regressions onto the (b) SAD, (c) AMO, and (d) PDO indices. The green boxes enclose the geographic regions of the Great Basin high (GBH) and Pacific subtropical high (PSH). The areas where the SLP-regressions are significant at the 95% confidence interval using a one-tailed t-test are dotted and only significant winds are shown. (e)–(h) As in (a)–(d), respectively, but for the latitudinal profiles of the 200 hPa zonal wind (U200; in m s^{-1}) averaged over 160°E–120°W. The dashed lines indicate the latitudinal center of the climatological U200. (i)–(l) As in (a)–(d), respectively, but for the standard deviations of the high-frequency (2–8 d) meridional wind at 250 hPa (V250; in m s^{-1}).

35°N (see figure 2(e)), which is consistent with the hypothesis.

The SLP anomalies regressed with both the AMO index (figure 2(c)) and the PDO index (figure 2(d)) show strong positive values over the Great Basin similar to the SAD-regression pattern, which indicates that the AMO and PDO can promote SAW activity via the GBH—pressure gradient mechanism. However, these two decadal modes produce opposite SLP anomalies over the subtropical Pacific; while the AMO strengthens the PSH, the PDO weakly weakens the PSH. With a stronger PSH, the AMO can cause the Pacific jetstream to displace more poleward and prevent winter cyclones from traveling through Southern California. The U200 anomalies regressed onto the AMO index (figure 2(g)) confirm that the Pacific jetstream is displaced about 10° more poleward from its climatological location. By regressing the std's of the high-frequency (2–8 d) winter meridional wind at 250 hPa onto the AMO index, we show in figure 2(k) that the maximum center of winter storm activity is displaced more northward compared to the climatology

(figure 2(i)). A similar displacement can also be seen in the regression onto the SAD index (figure 2(j)). As a result, the AMO can intensify SAW activity by strengthening the pressure gradient between the Great Basin and the Southern California coast and by simultaneously decreasing the hindering effect of winter cyclones on the SAW. In contrast, with a weakened PSH, the PDO can cause the Pacific jetstream to displace more southward (figure 2(h)) and bring more winter cyclones toward Southern California (figure 2(l)) to discourage the development of SAW. This southward displacement of the jetstream can cancel out the strengthening effect of the PDO on the SAW through the GBH—pressure gradient mechanism. The cancelation of these two mechanisms is the reason why the PDO has a weaker modulation effect on SAW activity than the AMO.

To further confirm the findings obtained from the 51 year long NCEP/NCAR Reanalysis dataset, we repeat the regression analysis using the 113 year long 20th century reanalysis dataset. The results confirm that the AMO strengthens both the GBH and PSH
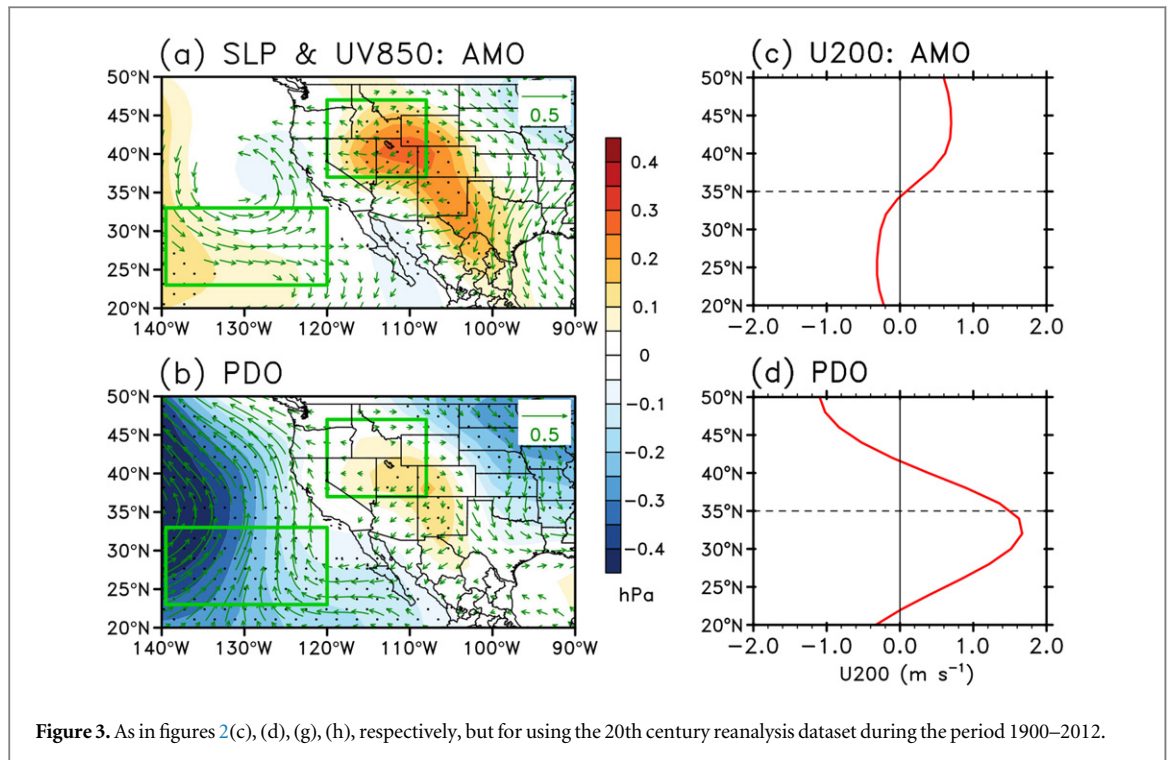
Figure 3. As in figures 2(c), (d), (g), (h), respectively, but for using the 20th century reanalysis dataset during the period 1900–2012.

(figure 3(a)) and displaces the jetstream more northward (figure 3(c)), while the PDO strengthens the GBH but weakens the PSH (figure 3(b)) and shifts the jetstream more southward (figure 3(d)).

3.3. The individual influences of the AMO and PDO during the three sub-periods of SAD variation

To confirm our suggestion that the AMO is more influential in modulating SAW activity than the PDO for the entire analysis period, we further examine the intensity of the SAD, AMO and PDO indices and their associated atmospheric circulation patterns for different time periods. Based on the discussion of figure 1, we divided the analysis period into three sub-periods: the first period in 1965–1982 (i.e., *P*1) where the SAD values are below normal and follow more of the AMO variation, the second period in 1983–1999 (i.e., *P*2) where the SAD values are above normal and follow more of the PDO variation, and the third period in 2000–2010 (i.e., *P*3) where the SAD values are above normal and follow the AMO variation again. During *P*1, the AMO stayed in the negative phase for the majority of this period while the PDO changed from a negative phase to a positive phase around 1976–77. The SAD variation in this period is more in-phase with the AMO index than the PDO index. The mean intensity (i.e., mean value) is –0.92 std's for the AMO index during this period and −0.64 std's for the PDO index. During *P*2, the PDO index is in the positive phase throughout while the AMO index changed from a negative phase to a positive phase in the early 1990s. In this period, the SAD variation is more in-phase with the PDO index. The mean intensity of the PDO index in this period is 1.02 std's, which is much stronger than

that of the AMO index (−0.11 std's). During *P*3, the AMO index stayed in the positive phase while the PDO index changed from a positive phase to a negative phase at the beginning of the period. At this time, the SAD variation is more in-phase with the AMO index. The mean intensity of the PDO index is very small (−0.08 std's) but the mean intensity of the AMO index is large (1.49 std's). It is apparent that the mean intensity of the AMO and PDO indices plays an important role in determining which index has a stronger control of the decadal variation of SAD. The decadal SAD variation is modulated more by the AMO during *P*1 and *P*3 when the AMO persistently stayed in one particular phase while, at the same time, the PDO changed its phase. The PDO took control of the SAD variation during *P*2 because the PDO persistently stayed in one particular phase while the AMO changed phases.

To identify the individual influences of the AMO and PDO in modulating the SAD variation, we reconstructed the anomalous atmospheric circulation patterns for these three sub-periods based on the mean intensity of the AMO and PDO indices. In figures 4(a)–(i), each of the SLP anomaly patterns is reconstructed by multiplying the SLP regression pattern (figures 2(b)–(d); obtained from the entire period) by the mean intensity of the index for each sub-period (figure 1). During *P*1, the reconstructed SLP pattern based on the SAD index (figure 4(a)) is characterized by strong negative anomalies over the Great Basin and the subtropical Pacific, which result in a weak SLP gradient to the Southern California coast and a weakened Pacific jetstream (figure 4(j)), which is consistent with the below-normal values of
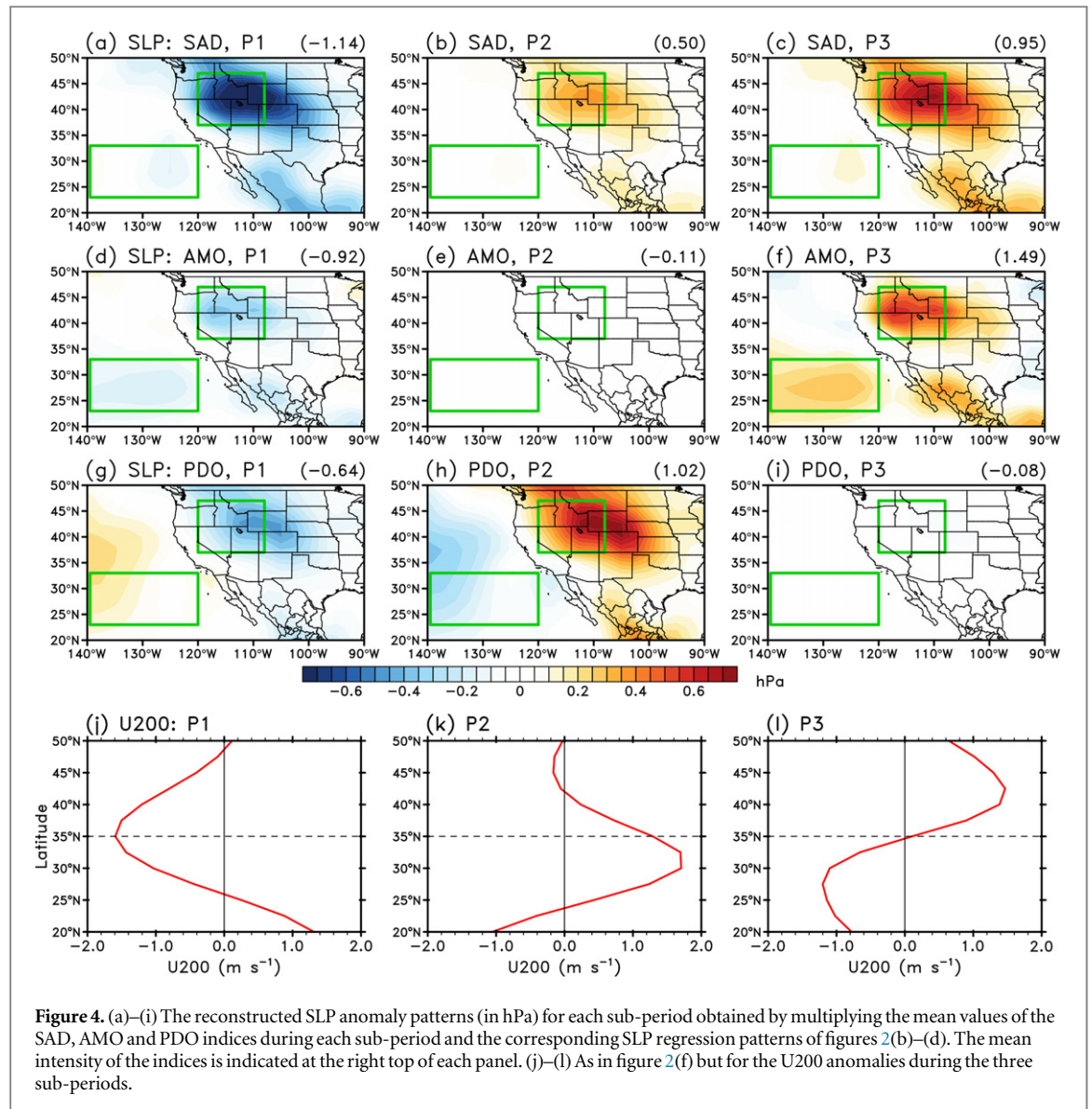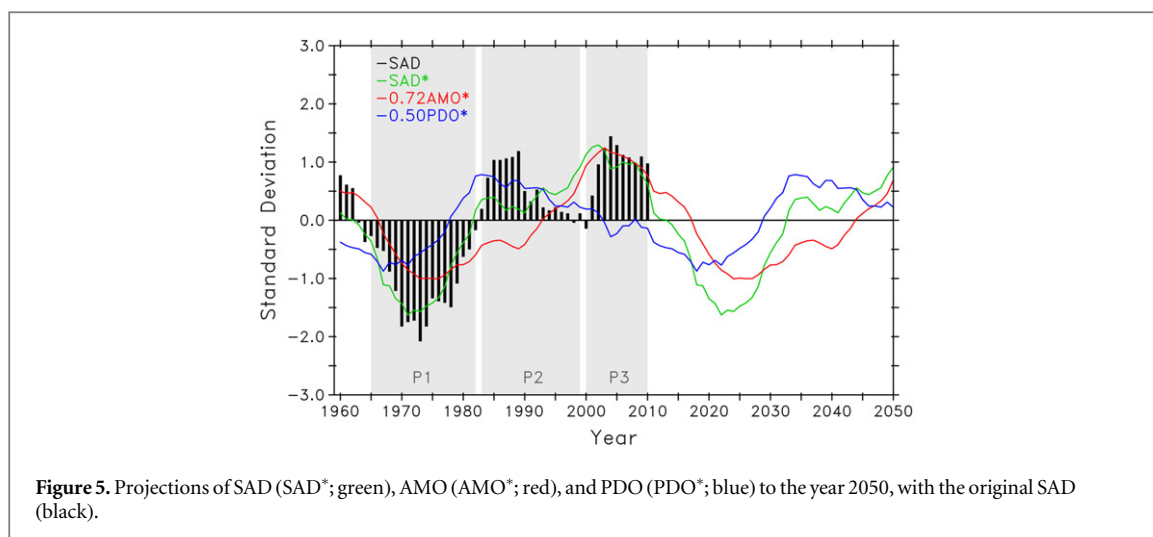
Figure 4. (a)–(i) The reconstructed SLP anomaly patterns (in hPa) for each sub-period obtained by multiplying the mean values of the SAD, AMO and PDO indices during each sub-period and the corresponding SLP regression patterns of figures 2(b)–(d). The mean intensity of the indices is indicated at the right top of each panel. (j)–(l) As in figure 2(f) but for the U200 anomalies during the three sub-periods.

the SAD observed in the period (see figure 1). The AMO-reconstructed SLP pattern (figure 4(d)) is similar to the SAD-reconstructed pattern (see figure 4(a)). The PDO-reconstructed SLP pattern (figure 4(g)) shows negative SLP anomalies over the Great Basin but positive SLP anomalies over the subtropical Pacific. While the former anomalies can weaken SAW activity, the latter anomalies can strengthen SAW activity. As a result, the PDO's influence on the SAW (and SAD) is weaker than the influence of the AMO. During *P*2, the SAD-reconstructed SLP pattern (figure 4(b)) has weak positive anomalies over the Great Basin but little influence on the PSH. The PDO-reconstructed SLP pattern (figure 4(h)) is in-phase with the SAD-reconstructed pattern, but the AMO-reconstructed SLP pattern (figure 4(e)) has very weak magnitude, making the PDO the main influence on the SAD variability in *P*2. However, a portion of the PDO's strengthening effect on the SAW through the Great Basin pressure gradient is canceled out by the PDO's weakening effect on the

SAW through the PSH, shifting the Pacific jetstream about 5° south from its climatological location (figure 4(k)). As a result, the mean intensity of the SAD index during this period (0.5 std's) is low. During *P*3, the SAD-reconstructed SLP pattern (figure 4(c)) also exhibits positive anomalies over the Great Basin and the subtropical Pacific with the above-normal SAD values. The magnitude of the AMO-reconstructed SLP pattern in *P*3 (figure 4(f)) is strongly positive, while the magnitude of the PDO-reconstructed SLP pattern (figure 4(i)) is very weak. Therefore, the AMO becomes the main influence on the SAD variability in this period. The U200 anomalies in figure 4(l) support this, showing that the jetstream is shifted more than 5° north of its climatological location, which would deflect mid-latitude cyclones away from Southern California, encouraging SAW development. This shift coincides with the high magnitude of the AMO-reconstructed SLP pattern in the subtropical Pacific (see figure 4(f)).

Figure 5. Projections of SAD (SAD*; green), AMO (AMO*; red), and PDO (PDO*; blue) to the year 2050, with the original SAD (black).

3.4. Future projections

The main findings we obtained from the past five decades of observation suggest that we can use the phase changes of the PDO and AMO to project how the SAD variability may behave in the coming few decades. This information, while not particularly accurate, can still be useful for city or state planning purposes. First, we applied the following multivariate linear regression model:

$$SAD^* = aAMO + bPDO \qquad (1)$$

for the 1960–2010 period to determine the regression coefficients (i.e., $a = 0.72$ and $b = 0.50$). We then extended the AMO and PDO indices to 2050 (i.e., AMO* and PDO*, respectively; see figure 5) using a Fourier decomposition. Lastly, we projected SAD (i.e., SAD*) by replacing the original time series (AMO and PDO) with the extended time series (AMO* and PDO*) in equation (1). As shown in figure 5, the SAD* (i.e., projected) variation matches up well with the SAD (i.e., original) variation during most of the analysis period (i.e., a correlation coefficient of 0.87; significant at the 99% level). Our projection indicates that the AMO* will shift to a negative phase after 2020 while the PDO* will continue to stay in the negative phase until the year 2030. Based on the projection, the above-normal SAW activity we observed in the most recent decade may be terminated after 2016. More importantly, the projection indicates that Southern California is expected to experience an extended period of below-normal SAW activity all the way to 2030.

4. Discussion and conclusion

In this study, we examined the decadal variation of the SAW activity and its connection with the decadal variability modes in the Pacific and Atlantic (i.e., the PDO and AMO) during 1960–2010. The correlation and regression analyzes using reanalysis datasets and climate indices revealed that the AMO has a stronger influence than the PDO on the decadal variability of the SAW through the GBH—pressure gradient mechanism and the PSH—jetstream displacement mechanism. The PDO and AMO are shown to have opposite modulation effects on the strength of the PSH and the consequent influence on SAW activity. It is the prediction of the North Atlantic ocean temperatures rather than the North Pacific ocean temperatures that are more relevant for projecting SAW activity and its associated impacts on Southern California in the coming decades. The changing influences of the PDO and AMO on the SAW revealed by this study have implications for the environment of Southern California, as wildfire frequency, SAW related air pollution episodes, and SAW-induced upwelling off the coast may change according to phases in the PDO and AMO. This study does not look into the physical processes that enable the AMO to influence the SLP variations over the Great Basin and the subtropical Pacific; however, prior studies have offered clues on the possible processes for the influence. For example, Zhang and Delworth (2007) suggested that the AMO can impact the North Pacific climate by altering the latitudinal location of the mid-latitude jetstream, while Yu *et al* (2015) and Gao *et al* (2016) noticed that the positive phase of the AMO can intensify the PSH. The mass redistribution associated with such a location shift and intensification may affect the strength of the SLP over the Great Basin and subtropical Pacific. Another issue not addressed in this study is the possible lagged relationship between the PDO and SAD, which may be related to the interdecadal modulation of the AMO to the PDO (Zhang and Delworth 2007). Further studies are needed to fully resolve these issues.

Acknowledgments

References

Abatzoglou J T, Barbero R and Nauslar N J 2013 Diagnosing Santa Ana winds in Southern California with synoptic-scale analysis *Weather Forecast.* **28** 704–10

Compo G P *et al* 2011 The twentieth century reanalysis project *Q. J. R. Meteorol. Soc.* **137** 1–28

Conil S and Hall A 2006 Local regimes of atmospheric variability: a case study of Southern California *J. Clim.* **19** 4308–25

Dettinger M D, Cayan D R, Diaz H F and Meko D M 1998 North–South patterns in Western North America on interannual-to-decadal timescales *J. Clim.* **11** 3095–111

Enfield D B, Mestas-Nuñez A M and Trimble P J 2001 The Atlantic multidecadal oscillation and its relation to rainfall and river flows in the continental US *Geophys. Res. Lett.* **28** 2077–80

Finley J and Raphael M 2007 The relationship between El Niño and the frequency and duration of the Santa Ana winds of Southern California *Prof. Geogr.* **59** 184–92

Gao T, Yu J Y and Paek H 2016 Impacts of four northern-hemisphere teleconnection patterns on atmospheric circulations over Eurasia and the Pacific *Theor. Appl. Climatol.* 1–17

Guazzotti S A, Whiteaker J R, Suess D, Coffee K R and Prather K A 2001 Real-time measurements of the chemical composition of size-resolved particles during a Santa Ana wind episode, California USA *Atmos. Environ.* **35** 3229–40

Hu H and Liu W T 2003 Oceanic thermal and biological responses to Santa Ana winds *Geophys. Res. Lett.* **30** 1596

Hughes M and Hall A 2010 Local and synoptic mechanisms causing Southern California's Santa Ana winds *Clim. Dyn.* **34** 847–57

Hughes M, Hall A and Kim J W 2009 *Anthropogenic Reduction of Santa Ana Winds.* CEC-500-2009-015-D California Climate Change Center pp 1–19

Hughes M, Hall A and Kim J 2011 Human-induced changes in wind, temperature and relative humidity during Santa Ana events *Clim. Change* **109** (Suppl. 1) 119–32

Jin Y, Randerson J T, Faivre N, Capps S, Hall A and Goulden M L 2014 Contrasting controls on wildland fires in Southern California during periods with and without Santa Ana winds *J. Geophys. Res. Biogeosci* **119** 432–50

Jones C, Fujioka F and Carvalho L M V 2010 Forecast skill of synoptic conditions associated with Santa Ana winds in Southern California *Mon. Weather Rev.* **138** 4528–41

Kalnay E *et al* 1996 The NCEP/NCAR 40 year reanalysis project *Bull. Am. Meteorol. Soc.* **77** 437–71

Kaplan A, Cane M, Kushnir Y, Clement A, Blumenthal M and Rajagopalan B 1998 Analyses of global sea surface temperature 1856–1991 *J. Geophys. Res.* **103** 18567–89

Kerr R A 2000 A North Atlantic climate pacemaker for the centuries *Science* **288** 1984–5

Langford A O, Pierce R B and Schultz P J 2015 Stratospheric intrusions, the Santa Ana winds, and wildland fires in Southern California *Geophys. Res. Lett.* **42** 6091–7

Mantua N J, Hare S R, Zhang Y, Wallace J M and Francis R C 1997 A Pacific interdecadal climate oscillation with impacts on Salmon production *Bull. Am. Meteorol. Soc.* **78** 1069–79

McCabe G J, Palecki M A and Betancourt J L 2004 Pacific and Atlantic Ocean influences on multidecadal drought frequency in the United States *Proc. Natl. Acad. Sci. USA* **101** 4136–41

Qian C, Yu J Y and Chen G 2014 Decadal summer drought frequency in China: the increasing influence of the Atlantic multi-decadal oscillation *Environ. Res. Lett.* **9** 124004

Raphael M N 2003 The Santa Ana winds of California *Earth Interact.* **7** 1–13

Raphael M and Mills G 1996 The role of mid-latitude Pacific cyclones in the winter precipitation of California *Prof. Geogr.* **48** 251–62

Schlesinger M E and Ramankutty N 1994 An oscillation in the global climate system of period 65–70 years *Nature* **367** 723–6

von Storch H and Zwiers F W 1999 *Statistical Analysis in Climate Research* (Cambridge: Cambridge University Press) p 494

Westerling A L, Cayan D R, Brown T J, Hall B L and Riddle L G 2004 Climate, Santa Ana winds and autumn wildfires in southern California *Eos Trans. AGU* **85** 289–96

Yu J Y, Kao P K, Paek H, Hsu H H, Hung C W, Lu M M and An S I 2015 Linking emergence of the Central-Pacific El Niño to the Atlantic multi-decadal oscillation *J. Clim.* **28** 651–62

Yue X, Mickley L J and Logan J A 2014 Projection of wildfire activity in southern California in the mid-twenty-first century *Clim. Dyn.* **43** 1973–91

Zhang R and Delworth T L 2007 Impact of the Atlantic multidecadal oscillation on North Pacific climate variability *Geophys. Res. Lett.* **34** L23708

Zhang Y, Wallace J M and Battisti D S 1997 ENSO-like interdecadal variability: 1900–93 *J. Clim.* **10** 1004–20